Corrosion Behavior of Chromatized Zinc-Electroplated Mild Steel

C.R. Valentini,‡, J. Fiora,** and A.M. Iglesias****

ABSTRACT

The electrochemical noise (EN) technique has been used to study the corrosion processes of mild steel substrate first coated with electrodeposited zinc, and then with a yellow chromate conversion coating treatment. The electrodes were tested in borate buffer solutions of pH 9.2. During the experiments, sodium chloride (NaCl) solutions were added to these solutions. After salt addition, current fluctuations of a smaller magnitude were observed, but only in one direction. Potential and current noise data were collected simultaneously. Before the statistical analysis, the recorded potential and current raw data were detrended by polynomial methods. Standard deviation of potential, current, and resistance noise were calculated. The standard deviation of noise resistance (calculated through potential and current measurement) allowed the detection of early changes on corrosion processes. Through the potential and current noise fluctuations, it was possible in this case to obtain valuable information to study the corrosion and protection mechanisms and thus to analyze the difference that appears between the processes carried out both in alkaline borate solutions and in alkaline borate solutions containing the aggressive chloride ion. There is not a good agreement between the corrosion rate values determined using the linear polarization technique and EN techniques. Kurtosis of potential (E_{Kurt}), current fluctuations (I_{Kurt}), and the ratio Kurtosis potential/Kurtosis current (E_{Kurt}/I_{Kurt}) were calculated.

KEY WORDS: chromate conversion coating, corrosion monitoring, electrochemical noise, zinc

INTRODUCTION

The electrolytic zinc plating is one of the alternatives to protect steel from the corrosion process. According to the position of the zinc and iron in the standard oxidizing potential table, when zinc is in contact with steel, a galvanic cell is formed, in which zinc is the anode. (In the presence of a corrosive environment, zinc is oxidized and oxides, hydroxides, and salts such as hydrozincite [$Zn_5(OH)_6(CO_3)_2$; usually named white corrosion] are formed). In the passivation of zinc, two types of surface oxidation products are formed when it is immersed in alkaline environments such as borate solutions. The outer layer is white, loose, and flocculent and is formed by precipitation from a supersaturated layer of zincate near the surface. The precipitated layer is formed by either zinc oxide (ZnO) or zinc hydroxide ($Zn[OH]_2$). The second film acts as a barrier layer, which forms directly from the metal Zn rather than by precipitation, and its formation is considered responsible for the transition from the active to the passive state.[1]

MacDonald, et al.,[1] suggested that the potential of zero thickness of the barrier layer, E_0, can be considered as the equilibrium potential of the zinc(II) oxide film on zinc:

Submitted for publication August 2006; in revised form, December 2007.

‡ Corresponding author. E-mail: cvalenti@inti.gov.ar.
* INTI – Procesos Superficiales, Edificio 46 (Parque Tecnológico Migueletes), Colectora de Avienda General Paz 5445, Casilla de Correo 157, B1650WAB San Martín, Buenos Aires, República Argentina.
** INTI – Energía, Instituto Nacional de Tecnología Industrial, Argentina.
*** Unidad de Actividad Química, Comisión Nacional de Energía Atómica, Argentina.

0010-9312/08/000159/$5.00+$0.50/0

$$ZnO + 2H^+ + 2e^- = Zn + H_2O \quad (1)$$

$$E_0 = -0.640 - 0.059\ pH\ vs.\ SCE \quad (2)$$

The potential of zero thickness can be determined from a graph of ZnO barrier layer thickness vs. oxide formation potential under steady-state conditions.

McKubre and Macdonald,[2] suggested that, in the prepassive region, the dissolution current is diminished by the presence of a three-dimensional porous film formed by $Zn(OH)_2$, which possibly reduces the effective surface area.

To prevent the early corrosion of zinc, pieces are usually treated with an oxidant chromic solution to obtain a conversion coating. In this way, it is possible to reach a passive state.

In a simplified form, the first reaction is a chromic attack of zinc in acid solution:

$$3Zn + 2CrO_4^{2-} + 10H^+ = 3ZnO + 2Cr^{3+} + 5H_2O \quad (3)$$

and the second reaction is:

$$2CrO_4^{2-} + 10H^+ + 6e^- = Cr_2O_3 + 5H_2O \quad (4)$$

In the chromium Pourbaix diagram,[3] it can be observed that the passivity range is notably reduced in the presence of chloride ions, and at pH 9.2, the chromium is out of the passive zone, where the chromium oxide/hydroxides are stable.

According to McCluskey,[4] the basis for corrosion protection of the chromate coating is due to the following two principle causes: barrier coating of zinc, which is related to the film thickness, and anodic protection due to Cr(VI).

To obtain an effective anodic protection, it is necessary to have water of hydration available for the reduction reaction; therefore, drying at temperatures higher than 70°C could eliminate this beneficial effect.

The electrochemical noise (EN) technique has been used to study corrosion processes since the early 1980s, and the sensitivity of the technique for the detection of spontaneous changes in corrosion processes was established. Mansfeld and Xiao[5] concluded that, at present, the EN technique can produce qualitative information concerning coating performance and, therefore, it is suited for corrosion-monitoring purposes.

In this paper, the corrosion behavior of chromatized zinc-electroplated mild steel in borate buffer solutions with and without the presence of chloride ions by means of the EN technique was studied.

EXPERIMENTAL PROCEDURES

Samples of mild steel substrate were taken from a rod with a diameter of 2.5 cm having the following nominal weight percentage composition: 0.04 C, 0.35 Mn, 0.023 P, 0.018 S, 0.08 Si, and balance Fe. After embedding the mild steel electrode in two components of epoxy resin, the total exposed surface area was 3.8 cm^2. The electrode surface was mechanically polished with consecutively finer grades of metallographic emery paper until emery grade 1000, and finally with particles of 2 μm diamond paste.

The polished mild steel was first coated with zinc electrodeposited from an alkaline, cyanide-free commercial bath at 0.063 A/cm^2 for 15 min. After the zinc deposition was concluded, the samples were rinsed with distilled water, immersed in 0.5% nitric acid (NHO_3) solution for 15 s, dipped in a commercial bath of yellow chromate conversion coating for 30 s, rinsed with water, and finally dried in an oven at a temperature of 60 ± 2°C. The average zinc thickness on the steel substrate was 8 μm. The thickness was measured using an x-ray fluorescence method.

Test solutions were made from analytical-grade reagents and distilled water. Borate buffer solutions of pH 9.2 + 1.0 × 10^{-3} M sodium sulfate (Na_2SO_4) were used at 25 ± 2°C. NaCl solution was added to these solutions during the experiments up to a concentration of 0.1 M in aerated conditions.

An electrochemical cell, machined from a polymethylmethacrylate resin bar, was used. Two identical samples were located parallel to each other in the electrolytic solution. A saturated calomel reference electrode (SCE) was placed between the two electrodes in the proximity of one of them by a Luggin capillary.

The current noise signal was amplified by means of an electronic circuit designed by the authors, and both current and potential noise were simultaneously recorded with a commercial acquisition data card system, controlled by a PC through commercial software.

The measurements were carried out for 24 h. The sampling rate was 2 points per second up to a total of 1,024 points, once every hour during a period of 24 h. In all the experiments, the samples were first immersed in the borate buffer solution, and during the second stage of the experiment, NaCl was added up to a concentration of 0.1 M.

Scanning electron micrographs were obtained from a scanning electron microscope. Specimens were previously cleaned in bidistilled water and ethanol (C_2H_6O), dried, and gold-coated. Additionally, the specimens were analyzed using energy-dispersive x-ray microanalysis (EDAX).

Linear polarization (LP) measurements were carried out with a potentiostat. A three-electrode electrochemical cell was used for the LP measurements. The counter electrode was a platinum sheet, the reference electrode was SCE, and the same electrode used in the EN measurements was used as the working electrode. The polarization curves were recorded in a potential range of ±20 mV around the corrosion potential, E_{corr}, at a scan rate of 0.1 mV/s. The polarization resistance, R_p, data was calculated.

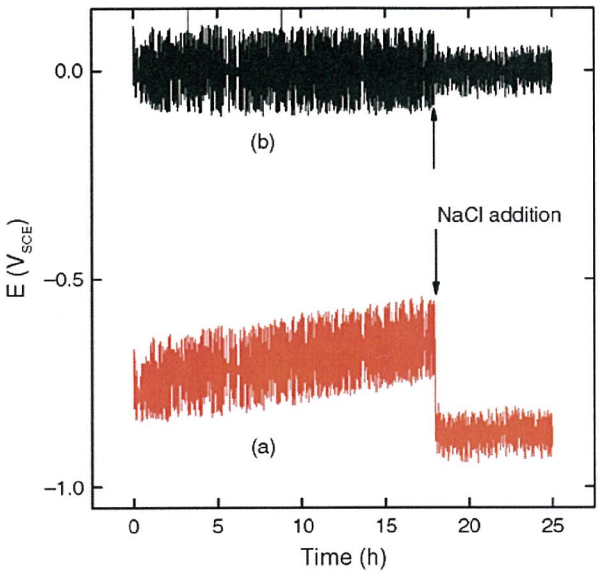

FIGURE 1. *Potential-time data for chromatized zinc-electroplated mild steel in borate buffer solution at pH 9.2 under two different conditions, before and after the addition of NaCl at about 18 h: (a) raw data and (b) after polynomial method detrending.*

METHODS OF ANALYSIS

For the analysis of EN, potential (E) and current (I) noise data must be collected simultaneously. The experimental approach for the collection of the EN data requires the use of two nominally identical working electrodes.

The calculated values of the standard deviations of the potential (σ_E) and current (σ_I) fluctuations, as well as the noise resistance, R_n,[6] taken from EN data, can be affected by drifts. Thus, the recorded current and potential raw data were detrended by polynomial methods.[7]

Potential and current noise were recorded in time and analyzed statistically from calculating the standard deviation.

The Kurtosis was calculated according to the following equation:

$$\kappa_{Kurt} = \left\{ \frac{n(n+1)}{(n-1)(n-2)(n-3)} \sum \left(\frac{x_j - \bar{x}}{\sigma} \right)^4 \right\} - \frac{3(n-1)^2}{(n-2)(n-3)} \quad (5)$$

where $\bar{x}$ is the mean value of E or I; x_j is the value of E or I; κ_{Kurt} is E or I Kurtosis.

The Kurtosis is a measure of whether the data are peaked or flat relative to a normal distribution. A positive Kurtosis value suggests a relatively peaked distribution, while a negative Kurtosis indicate a relatively flat distribution.[8]

[1] UNS numbers are listed in *Metals and Alloys in the Unified Numbering System*, published by the Society of Automotive Engineers (SAE International) and cosponsored by ASTM International.

The Kurtosis values for the potential and current signals are sensitive indicators of changes in corrosion rate and mechanisms.[9]

The R_n was calculated as the ratio between σ_E and σ_I. The values of R_n can be compared with the R_p, so that the corrosion rate can be deduced by means of the Stern-Geary relationship.[10] Chen and Bogaerts showed that in certain circumstances (i.e., reactions are activation-controlled; electrode potential is far from the equilibrium potential; and the reaction is in a steady-state condition) the R_n is indeed equivalent to the R_p.[11] However, Mansfeld, et al., for the passive system Type 316L (UNS S31603)[1] stainless steel (SS)/Ringer's solution, found that R_n was much smaller than R_p.[12]

The corrosion rate (I_{corr}), applying the Stern-Geary equation, was calculated according to:

$$I_{corr} = \frac{B}{R_p} \quad (6)$$

$$B = \frac{b_a b_c}{2.3(b_a + b_c)} \quad (7)$$

where b_a and b_c are the anodic and cathodic Tafel constants.

RESULTS AND DISCUSSION

In Figure 1(a), the potential-time raw data obtained in the borate buffer solution are shown under two different conditions: before and after the addition of NaCl at about 18 h. Before the addition of NaCl, the electrode potential fluctuates at around –0.65 V. After adding the NaCl solution, the potential abruptly varies to a value of around –0.9 V, and the amplitude of the potential fluctuations results are smaller than that observed before the addition of the chloride ions.

Figure 1(b) shows the detrended potential-time data, where the potential is uniformly distributed around 0 V and the potential drift has been eliminated. As a consequence of this data treatment, important information about the corrosion processes provided by the electrode potential value is lost.

Both fluctuations of electrode potential and its variation in the mean value observed after adding NaCl can be explained with the consideration of the reactions that take place in the corrosion process. Before the addition of NaCl, a mix potential is established in the electrode as a consequence of two different possible anodic reactions: the Zn and Cr oxidation. According to Pourbaix,[3] the most thermodynamically stable oxidation state for Cr is +2, and thus the following hemi-reactions can be proposed:

$$2Cr^{2+} + 3H_2O = Cr_2O_3(c) + 6H^+ + 2\,e^- \quad (8)$$
$$E = -1.05\ V_{NHE} \text{ at pH } 9.2$$

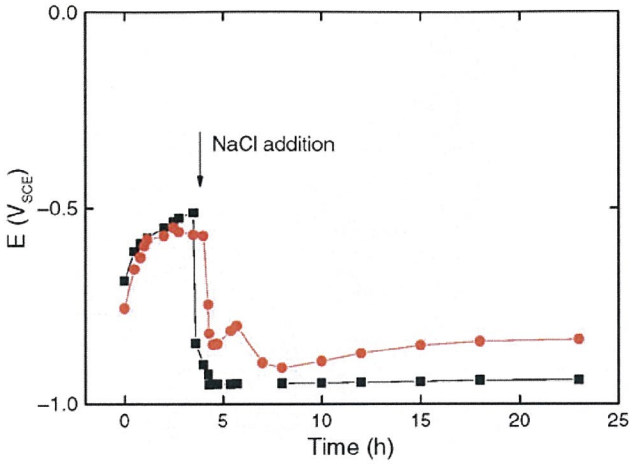

FIGURE 2. *Potential vs. time curves for (■) mossy Zn electrode in buffer borate solution at pH 9.2 and 25°C before and after 0.1 M NaCl addition and (●) mild steel substrate/Zn/yellow chromate coating in the same electrolyte conditions.*

$$Zn = Zn^{2+} + 2e^- \qquad E = -0.7618\ V_{NHE} = -1.0091\ V_{SCE} \tag{9}$$

The cathodic reaction is oxygen reduction:

$$O_2 + 2H_2O + 4e^- = 4OH^- \qquad E = -0.401\ V_{NHE} = -0.642\ V_{SCE} \tag{10}$$

The observed mix potential was close to –0.65 V; this value is consistent with those obtained from the thermodynamic equilibrium of equations (Equation [10] cathodic reaction).

When the NaCl solution is added, the electrode potential changes to a value around –0.9 V, and the electrode potential fluctuations are smaller in amplitude with respect to the previous situation to the salt addition.

Equation (8) could be one of the redox reactions that promote the Cr depassivation by the chloride action. Nevertheless, it can be seen in the Pourbaix diagram[3] that there are several possible reactions for the Cr. In Figure 2, during the experiment with the mossy Zn electrode in the buffer borate solution at pH 9.2 and 25°C, it is possible to observe the following evolution: in the beginning of the experiment the pure Zn grit potential increased from –0.75 V_{SCE} to –0.5 V_{SCE} after 5 h. When the NaCl solution is added up to a concentration of 0.1 M in the aerated condition, the mossy Zn grit potential electrode falls rapidly and at –0.94 V_{SCE} is stabilized (–1.18 V_{NHE}).

The initial potential evolution, before the chlorine addition, could be attributed at the formation of a ZnO film. According to Macdonald, et al.,[1] this film grows up to a certain thickness, which, if it was compared with the experiment realized by them at pH 10.5, a thickness circa of 0.6 nm could be obtained.

After chlorine is added, the electrode potential can be compared with those from the following reactions:

$$Zn = Zn^{2+} + 2e^- \qquad E = -0.986\ V_{NHE} \tag{11}$$

This potential was calculated at pH 9.2 using the solubility product constant, K_{ps}, to assign a Zn(II) concentration in the solution.

$$Zn + 4OH^- = ZnO_2^{2-} + 2H_2O + 2e^- \qquad E = -1.109\ V_{ENH} \text{ using the corresponding equilibrium}^4 \tag{12}$$

$$Zn + 2OH^- = Zn(OH)_2 + 2e^- \qquad E = -0.962\ V_{NHE}{}^1 \tag{13}$$

On the other hand, with a chloride concentration of 0.1 M and pH 9.2, in the diagram log[activity] vs. pH,[13] the thermodynamically stable phase is ε $Zn(OH)_2$ and the ionic species are $ZnOH^+$, $Zn(OH)_3^-$, and Zn^{2+}, respectively.

In one of the experiments, the coating was detached in only one of the two electrodes after the electrochemical noise experiments in chloride medium. In spite of the objective to obtain a homogeneous solution in chloride, it is very probable that, initially, when the chloride is added, the chloride concentration is not distributed homogeneously in the solution bulk. In these conditions, during the homogenization process, one of the electrodes could receive preferentially a considerable chloride concentration, which determines the formation of concentration cells. Two processes appeared: an attack of the chloride ions preferentially to one of the working electrodes and a slow process of diffusion to homogenize the chloride concentration of the solution in the cell. For this reason, one of the working electrodes develops preferably an anodic reaction, leaving the other electrode to act as the cathode. The experiment was repeated with similar results.

The detached coating sample after being in contact first with the borate solutions and then with the NaCl solution, to identify the corrosion origin site, was removed from the electrochemical cell, dried, and examined using SEM and EDAX. Figure 3(a) shows that the electrode surface presents cracks and smooth regions (plaques). Some cracks were attacked while others were not. Figures 3(b) and (c) show an EDAX average elemental Zn and Cr mapping in the same electrode area presented in Figure 3(a). Table 1 shows the semiquantitative composition realized by EDAX on the surface coating inside one of the cracks and one of the plaques, respectively. In the crack, the Cr weight percentage concentration is about 3% and the Zn weight percentage concentration is about 93%. In the plaque, the Cr weight percentage concentration is 10.5% and the Zn weight percentage concentration is 87%. This means that, from the corrosion point

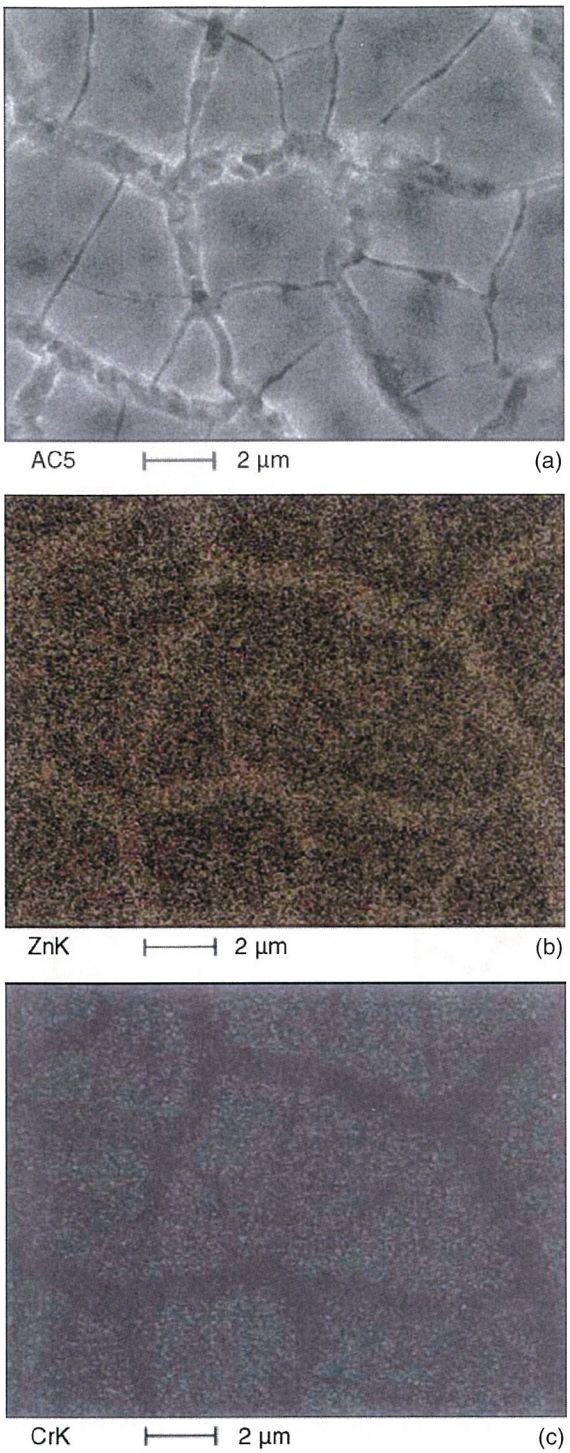

FIGURE 3. *(a) SEM micrographs of the electrode surface presenting cracks and smooth regions (plaques), (b) EDAX average elemental Zn mapping of the same area of the electrode, and (c) EDAX average elemental Cr mapping in the same area.*

of view, in the crack region, where the Cr concentration is smaller than in the plaques, the action of the Cr_2O_3 oxides is diminished and the zone is less protected.

TABLE 1
Energy-Dispersive X-Ray Microanalysis

	Concentration (% p/p) Plaques	Concentration (% p/p) Cracks
Cr	10.5	3.0
Fe	2.9	2.84
Zn	86.6	92.98
Si	—	1.18

The results presented in Figure 2 seem to support the idea that the anodic process is governed by Zn oxidation. In this figure, the potential evolution vs. time of a pure zinc electrode is shown together with an electrode of mild steel substrate/zinc/yellow chromate coating in a buffer borate solution at pH 9.2 and 25°C, before and after the addition of chloride ion up to a 0.1 M concentration. When the NaCl solution is added, a decrease of around 300 mV in the potential is observed in both electrodes. The similitude in the behavior of both electrodes strongly suggests that the conversion coating does not affect the zinc probe potential. It is worth noting that the abrupt potential change is the same magnitude of that observed during the electrochemical noise experiments.

The fact that the potential noise range diminished when the chloride ion was added can be explained because the system is controlled by a redox reaction that has a low resistance. In this condition, the potential does not oscillate between the zinc corrosion process and the oxygen discharge reaction (polarization of electrodes).

When a potential measurement is carried out with a ordinary voltmeter, the result of the measurement is in general the average of a burst of potential measurement; however, the EN technique is able to record the fast potential fluctuations that take place during the corrosion processes.

The current noise of the raw data vs. time can be seen in Figure 4(a). During the first stage of the experiment, positive and negative fluctuating values of current, with an amplitude of around 4×10^{-4} A, were recorded. After NaCl solution was added, the current had fluctuations of only one sign (positive in this case) and the amplitude was approximately 1×10^{-4} A.

When the chloride ion is added, the decrease of the current fluctuation amplitude can be explained in terms of the acceleration of the corrosion processes promoted by the chloride ion, diminishing the barrier layer thickness. On the other hand, the precipitated layer of ZnO and $Zn(OH)_2$, which form the white corrosion products, blocks the active sites for the anodic process and thus promotes the decrease of the current noise amplitude.

The observation of current noise of only one sign, in the case that one of the electrodes is attacked and loses part of the coating after the chloride ion addition, is very similar to the process of galvanic coupling

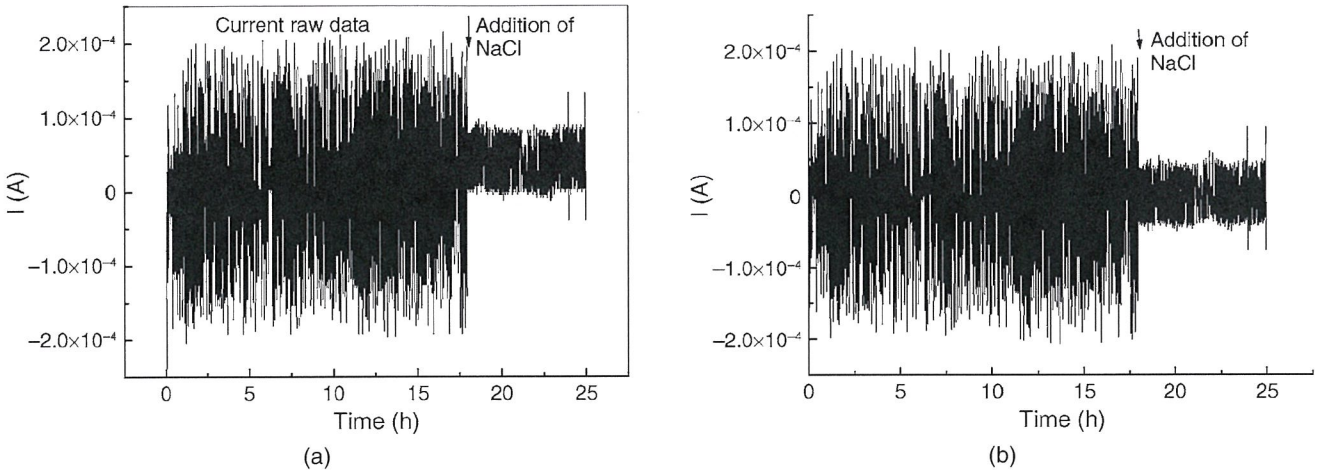

FIGURE 4. *Current-time data for chromatized zinc-electroplated mild steel in borate buffer solution at pH 9.2 under two different conditions, before and after the addition of NaCl at about 18 h: (a) raw data and (b) after polynomial method detrending.*

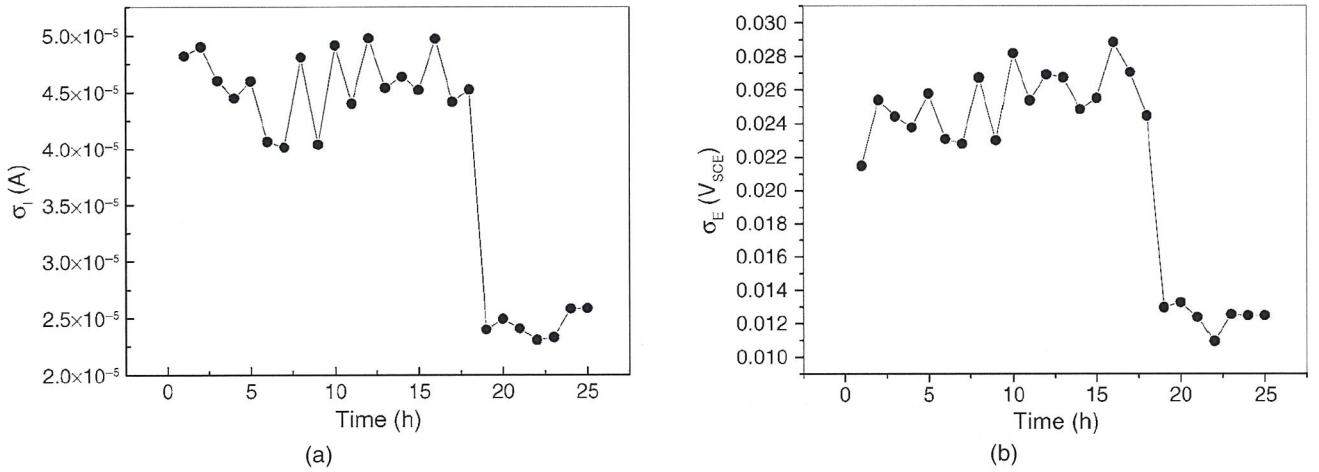

FIGURE 5. *Time evolution of (a) current noise standard deviation and (b) potential noise standard deviation.*

between two metals, in which one of them is more noble than the other. The oxidation process is always produced at the less noble metal and the current is observed in only one direction.

Figure 4(b) shows the data presented in Figure 4(a) after subtracting the drift by a polynomial method. The current noise is uniformly distributed around null current. However, the important information related to the sign of the current noise is lost when the drift is removed.

Figure 5(a) shows the curve of standard deviation current noise, σ_I, vs. time. During the first step of the experiment, the σ_I values were in the range from 4×10^{-5} A to 5×10^{-5} A. When NaCl was added, at around 18 h of the running experiment, both σ_I values were about 2.5×10^{-5} A, and at the same time, the fluctuation amplitude of σ_I values decreased. The main ideas given for the behavior of σ_I vs. time are the same that were used to explain the variations of current vs. time shown in Figure 4(a).

The time evolution of the potential noise standard deviation, σ_E, can be seen in Figure 5(b). During the first stage of the experiment, the curve σ_E vs. time shows oscillations of σ_E in the range of about 26 mV. When the NaCl solution was added, a sudden decrease of σ_E at about 12 mV occurred.

The time evolution of the R_n can be seen in Figure 6. The R_n values do not show practically any important change before and after the chloride ion was added, in which the average R_n values stayed at about 5.6×10^2 Ω. That means the R_n does not distinguish any change in the corrosion process.

The time evolution of current noise Kurtosis (I_{Kurt}), potential noise Kurtosis (E_{Kurt}), and the ratio potential noise Kurtosis/current noise Kurtosis (E_{Kurt}/I_{Kurt}) can be seen in Figure 7. During the first step of the exper-

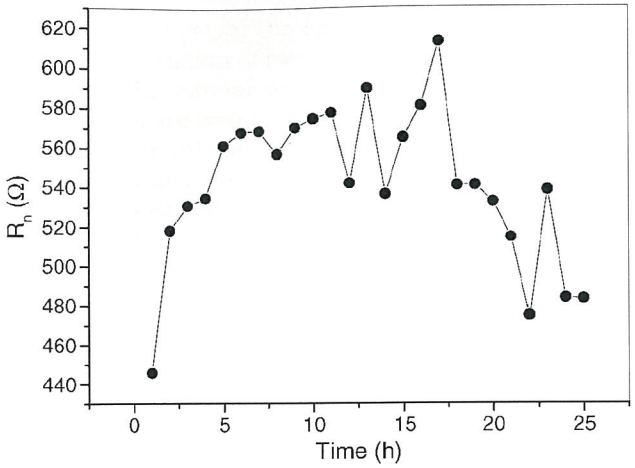

FIGURE 6. *Time evolution vs. noise resistance.*

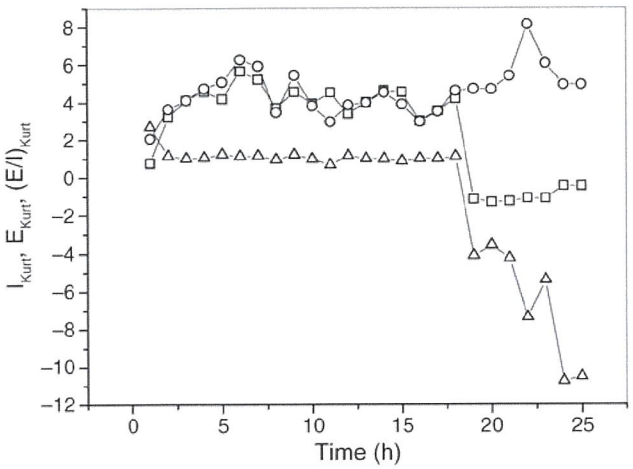

FIGURE 7. *(□) Time evolution vs. current noise Kurtosis, (○) potential noise Kurtosis, (△) and ratio potential noise Kurtosis/current noise Kurtosis.*

iment, both curves E_{Kurt} and I_{Kurt}, respectively, present Kurtosis oscillations around 5. When the chloride ion is added, a significant change is observed by which E_{Kurt} grows in an abrupt form, but I_{Kurt} diminishes in the same form. During the first step of the experiment, the ratio E_{Kurt}/I_{Kurt} remains practically constant around 1, and after the chloride ion is added, an abrupt drop was observed, which means the ratio E_{Kurt}/I_{Kurt} revealed the change of corrosion process.

In Table 2, the corrosion rate data determined by both EN and LP techniques are compared with those obtained from the references. In the system steel/zinc/yellow chromate conversion coating in a buffer borate solution, pH 9.2 + 1.0×10^{-3} M Na_2SO_4 at 25 ± 2°C, the R_n value is three orders smaller than R_p values. Similar results were reported by Mansfeld, et al.,[12] for the passive system Type 316L SS/Ringer's solution, by which R_n resulted in two orders smaller than R_p. These results suggest that, to calculate the corrosion rate, if we assume that $R_n = R_p$, the result of the corrosion rate in this case would be overestimated. In Table 2, an example can be seen by which to calculate the corrosion rate with the Stern-Geary equation, where $R_n = R_p$ and B = 0.0018 mV.[14] In the system steel/zinc/yellow chromate conversion coating in the buffer borate solution at pH 9.2 + 1.0×10^{-3} M Na_2SO_4 at 25 ± 2°C, $R_n = 5.8 \times 10^2$ Ω, and the corrosion rate is 8.2×10^{-6} A/cm^2. On the other hand, the corrosion rate value calculated from $R_p = 1.4 \times 10^5$ Ω is 3.4 10^{-8} A/cm^2, which means the corrosion rate obtained from EN technique is 2 orders larger than that calculated from the LP technique. These results are in disagreement with the work of Chen and Bogaerts,[11] who showed an equality between R_n and R_p, and Torres, et al.,[15] who reported that from pH 1 to pH 14, there is a good agreement between both resistances (R_n and R_p) for steel and stainless steel. In this last work, important variations appear when compared to

TABLE 2

Comparative Values of Corrosion Rate, Noise Resistance, and Polarization Resistance

System	Noise Resistance, R_n (Ω)	Linear Polarization Resistance, R_p (Ω)	Corrosion Rate (A/cm^2)
Steel/zinc/yellow chromate conversion coating in buffer borate solution pH 9.2 + 1.0×10^{-3} M Na_2SO_4 at 25°C ± 2°C	5.8×10^2		8.2×10^{-6}
Steel/zinc/yellow chromate conversion coating in buffer borate solution pH 9.2 + 1.0×10^{-3} M Na_2SO_4 + 0.1 M NaCl at 25°C ± 2°C	5×10^2		9.5×10^{-6}
Steel/zinc in buffer borate solution pH 9.2 + 1.0×10^{-3} M Na_2SO_4 at 25°C ± 2°C	6.2×10^2		7.6×10^{-6}
Steel/zinc in buffer borate solution pH 9.2 + 1.0×10^{-3} M Na_2SO_4 at 25°C ± 2°C		1.4×10^5	3.4×10^{-8}
Steel/zinc/yellow chromate conversion coating in buffer borate solution pH 9.2 + 1.0×10^{-3} M Na_2SO_4 at 25°C ± 2°C		1.4×10^5	3.4×10^{-8}
Zn coating in 3% NaCl solution[14]			3.4×10^{-6}
Zn in soils[16]			From 2.8×10^{-8} to 2.1×10^{-6}
Zn in seawaters[16]			From 7.5×10^{-7} to 2.9×10^{-6}

the values obtained for the carbon steel at pH 4 and pH 5 with a variation of two orders of magnitude in both R_p and R_n. Similar behavior appears when the R_n and R_p values are compared at pH 1 and pH 2. This means that the pH value determines the corrosion behavior, as it was predicted by Pourbaix diagrams.

On the other hand, when the Zn behavior was analyzed by Macdonald, et al.,[1] they mentioned the existence of a local change in pH. It was then possible to attribute these changes to the differences in the R_n and R_p values obtained, because the EN experiment takes 24 h (in this period the oxide film developed on the surface electrode). On the other hand, the LP technique takes a few minutes and does not allow the the oxide film to develop on the surface electrode.

For the system steel/zinc coating and steel/zinc/yellow chromate conversion coating in the buffer borate solution, pH 9.2 + 1.0×10^{-3} M Na_2SO_4 at 25 ± 2°C, the R_p values are of the same order (1.4×10^5 Ω). As a consequence, the chromate conversion coating does not reduce the corrosion rate (3.4×10^{-8} A/cm^2) in the buffer solution.

As can be seen in Table 2, in the system steel/zinc/yellow chromate conversion coating in the buffer borate solution, pH 9.2 + 1.0×10^{-3} M Na_2SO_4 at 25 ± 2°C + 0.1 M NaCl solution, the R_n value is 5.8×10^2 Ω (that means 8.2×10^{-6} A/cm^2) and in steel/Zn in the same electrolyte, R_n is 6.2×10^2 Ω (7.6×10^{-6} A/cm^2). According to these results, from the corrosion point of view, both techniques EN and LP proved that the chromate conversion coating in the studied case does not produce additional protection.

In Table 2, for the system Zn coating in 3% NaCl solution,[14] the corrosion rate reported from the references (3.4×10^{-6} A/cm^2) is the same order as that in the system steel/zinc/yellow chromate conversion coating in buffer, pH 9.2 + 1.0×10^{-3} M Na_2SO_4 at 25 ± 2°C + 0.1 M NaCl solution (9.5×10^{-6} A/cm^2) obtained from the EN technique.

CONCLUSIONS

❖ The polynomial method of removing the drift from the recording potential and current noise contributes to the data treatment, but masks the potential step, which allows the changes in the reactions that take place on the electrodes to be seen.

❖ The SEM analysis of the samples shows that the attack in the presence of chloride ions occurs preferably in the cracks (edges of the plaques), and this is due to the following: the mechanical stress of the coating in the cracks and the lesser amount of chromium detected in the crack. Taking into account the Pourbaix diagram, the result is reasonable because the chromium is not a passive film in the presence of chloride ions at pH 9.2.

❖ Both the electrochemical noise and the resistance polarization techniques show that the chromate conversion coating on Zn surfaces in a medium-like buffer borate solution at pH 9.2 does not perform any protective effect.

❖ The R_n values were three orders smaller than R_p values. Similar results were reported by Mansfeld, et al.,[12] for the passive system Type 316L SS/Ringer's solution.

❖ It is necessary not to overestimate the corrosion rate when it is assumed that R_n is equal to R_p. The corrosion rate values using LP and EN techniques are in the range of the reference data.

❖ The decrease of the amplitude in the current fluctuations is a clear signal of the introduction of the chloride ions on the surface film, the so-called "white corrosion" that appears and covers the pores and thus makes it difficult for the arrival of the reactive to the active surface, as suggested by McKubre and Macdonald.[2]

❖ According to our results, chromate conversion coating does not seem to improve the corrosion resistance behavior of Zn/steel in the studied medium, in opposition to what was found in other conditions.[4]

ACKNOWLEDGMENTS

The authors acknowledge M. del Carmen Raffo from Unidad de Actividad Química, Comisión Nacional de Energía Atómica, Argentina, and G. Ybarra of INTI – Procesos Superficiales, Instituto Nacional de Tecnología Industrial, Argentina, for their useful discussions.

REFERENCES

1. D.D. Macdonald, K.M. Ismail. E. Sikora, *J. Electrochem. Soc.* 145, 9 (1998).
2. M.C.H. McKubre, D.D. Macdonald, *J. Electrochem. Soc.* 128, 3 (1981): p. 524-530.
3. M. Pourbaix, *Atlas of Electrochemical Equilibria in Aqueous Solutions* (Houston, TX: NACE International, 1974), p. 265.
4. P. McCluskey, *Trans IMF* 74, 4 (1996): p. 119.
5. F. Mansfeld, H. Xiao, "Electrochemical Noise Measurement for Corrosion Applications," ASTM 1277 (West Conshohocken, PA: ASTM International, 1996), p. 59-78.
6. F. Mansfeld, Z. Sun, C.H. Hsu, A. Nagiub, *Corros. Sci.* 43, 2 (2001): p. 341-352.
7. U. Bertocci, F. Huet, R.P. Nogueira, P. Rousseau, *Corrosion* 58, 4 (2002): p. 337-347.
8. H.E. Hill, J.W. Prane, *Applied Techniques in Statistics for Selected Industries* (New York, NY: John Wiley & Sons, Inc., 1984), p. 20.
9. D.A. Eden, "Electrochemical Noise: The First Two Octaves," CORROSION/98, paper no. 386 (Houston, TX: NACE, 1998).
10. J.R .Kearns, J.R. Scully, P.R. Roberge, D.L. Reichert, J.L. Dawson, eds., "Electrochemical Noise Measurement for Corrosion Applications," STP 1277 (West Conshohocken, PA: ASTM International, 1996).
11. J.F. Chen, W.F. Bogaerts, *Corros. Sci.* 37 (1995): p. 1,839-1,842.
12. F. Mansfeld, Z. Sun, C.H. Hsu, *Electrochim. Acta* 46 (2001): p. 3,651-3,664.
13. X.G. Zhang, *Corrosion and Electrochemistry of Zinc* (New York, NY: Plenum Press), p. 22-23.
14. L.A.S. Silva, L. Sathler, *Plat. Surf. Finish.* 11 (2003): p. 38-42.
15. A. Torres, J. Uruchurtu, J.G. González Rodríguez, S. Serna, *Corrosion* 63, 9 (2007): p. 866-871.
16. X.G. Zhang, *Corrosion* 55, 8 (1999): p. 788-794.
17. M.G. Kendall, *The Advanced Theory of Statistics* (London, U.K.: Charles Griffin & Company Limited, 1952), p. 142.

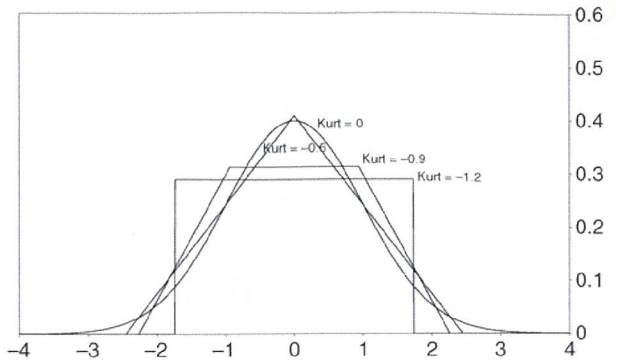

FIGURE A-1. *Normal distribution (Kurtosis zero) and "trapezoidal" distributions (negative Kurtosis).*

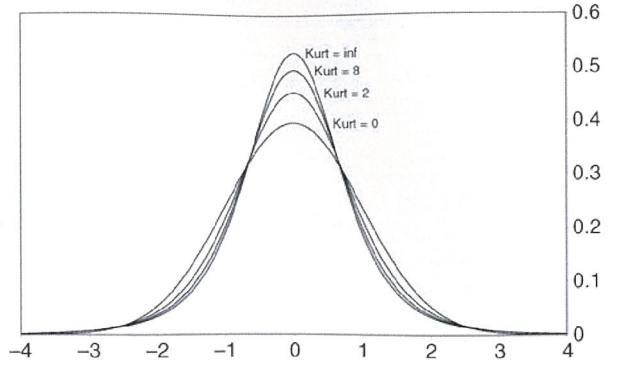

FIGURE A-2. *Normal distribution (Kurtosis zero) and Pearson-type VI distributions[17] (positive Kurtosis).*

APPENDIX

Kurtosis

The fourth moment about the mean is given by the following equation:

$$\mu_4 = \int_{-\infty}^{+\infty} f(x)(x-\mu)^4 dx \qquad \text{(A-1)}$$

where f is the probability density function and μ is the mean value.

Although, Kurtosis is more commonly defined as:

$$\kappa = \frac{\mu_4}{\sigma^4} - 3 \qquad \text{(A-2)}$$

where σ is the standard deviation.

As was pointed out in the paper, Kurtosis is a measure of whether the data are peaked or flat relative to a normal distribution.

Notice that all the members of the family of distribution of probabilities, $f_a(x) = \frac{1}{a} f\left(\frac{1}{a}\right)$, have the same kurtosis value, because the fourth moment about the mean and the fourth power of the standard deviation are both proportional to a^4.

In Figures A-1 and A-2, curves of positive and negative Kurtosis are shown, all of them with unit standard deviation. In Figure A-1, distributions with negative Kurtosis of 0, −0.6, −0.9, and −1.2, respectively, are shown, which have a flatter distribution. Finally, in Figure A-2, distributions with positive Kurtosis values of 0.2, 8, and ∞, respectively, are shown. The more kurtosis they have, the more peaked they are.